Chapter 8
Quantum Hardware II: cQED and cirQED

8.1 Introduction

In a vacuum, which contains no free charges or currents, electric $\vec{E}(x, y, z, t)$ and magnetic $\vec{B}(x, y, z, t)$ fields obey the following Maxwell equations (in Gaussian units)

$$
\begin{aligned}
&(I) \quad \frac{\partial E_x}{\partial x} + \frac{\partial E_y}{\partial y} + \frac{\partial E_z}{\partial z} = 0 \\
&(II) \quad \frac{\partial B_x}{\partial x} + \frac{\partial B_y}{\partial y} + \frac{\partial B_z}{\partial z} = 0 \\
&(III) \quad \frac{\partial E_z}{\partial y} - \frac{\partial E_y}{\partial z} + \frac{\dot{B}_x}{c} = \frac{\partial E_x}{\partial z} - \frac{\partial E_z}{\partial x} + \frac{\dot{B}_y}{c} = \frac{\partial E_y}{\partial x} - \frac{\partial E_x}{\partial y} + \frac{\dot{B}_z}{c} = 0 \\
&(IV) \quad \frac{\partial B_z}{\partial y} - \frac{\partial B_y}{\partial z} - \frac{\dot{E}_x}{c} = \frac{\partial B_x}{\partial z} - \frac{\partial B_z}{\partial x} - \frac{\dot{E}_y}{c} = \frac{\partial B_y}{\partial x} - \frac{\partial B_x}{\partial y} - \frac{\dot{E}_z}{c} = 0.
\end{aligned}
\tag{8.1}
$$

Here c is the speed of light in the vacuum, and we used Newton's dot notation to denote time derivatives. Let's consider the following ansatz for the electric $\vec{E}(z, t) = \hat{\mathbf{i}}\, E(z, t)$ and magnetic $\vec{B}(z, t) = \hat{\mathbf{j}}\, B(z, t)$ fields

$$
\begin{aligned}
B(z, t) &= a(t)\, k\, \exp(\mathrm{i}(k\, z - \pi/2)) + h.c. \\
E(z, t) &= \dot{a}(t)/c\, \exp(\mathrm{i}k\, z) + h.c
\end{aligned}
\tag{8.2}
$$

where $a(t)$ is a complex function of time t, k is a real number and $h.c.$ is the complex conjugate of the latter term. Plugging (8.2) into (8.1) we find that equations (I) and

B. Zygelman, *A First Introduction to Quantum Computing and Information*,
https://doi.org/10.1007/978-3-319-91629-3_8

(II) are immediately satisfied as both $\vec{E}$ and $\vec{B}$ are functions of z and have no vector components in the z-direction. Condition (III) is also satisfied but (IV) requires that

$$\ddot{a}(t) + k^2 c^2 \, a(t) = 0. \tag{8.3}$$

We recognize (8.3) as the equation of motion for a simple harmonic oscillator. Its solutions are $a(t) = a_\omega \, exp(\pm \mathrm{i} \, \omega \, t)$ where a_ω is a complex constant and $\omega = kc$. The time average, $< \vec{S} >$, over a single period $2\pi/\omega$, of the Poynting vector [1]

$$\vec{S} \equiv \frac{c}{4\pi} \, \vec{E} \times \vec{B} \tag{8.4}$$

denotes an energy current (i.e., it has units of energy/area/time), and if $a(t) = a_\omega \, exp(-\mathrm{i}\omega t)$,

$$< \vec{S} >= |a_\omega|^2 \frac{\omega}{c} \, \hat{k}. \tag{8.5}$$

Thus (8.2) represents an electromagnetic wave that transmits energy along the z-axis. For that wave, k is the wavenumber, and it is related to its wavelength $\lambda = 2\pi/k$; the distance by which the phase changes, at a single instance of time, from 0 to 2π. The rate of change of the phase at a given point in space is called the phase velocity and is here given by the speed of light c.

Now let's explore how these fields are modified in a setup in which two large parallel (perfectly) conducting plates in the xy plane are situated at $z = 0$ and $z = d$ on the propagation axis. Though fields (8.2) satisfy Maxwell's equations, they do not satisfy boundary conditions (b.c.) at the plates. We require b.c. so that $\vec{E}(0, t) = \vec{E}(d, t) = 0$ [1]. Consider the condition at $z = 0$, (8.2) stipulates that

$$E(0, t) \equiv E^+(0, t) = -\mathrm{i}\frac{\omega}{c} \left(a_\omega \exp(-\mathrm{i}\omega \, t) - a^*_\omega \exp(\mathrm{i}\omega \, t)\right)$$

and so the boundary condition is not met for arbitrary values of t. Now,

$$E^-(z, t) = \mathrm{i}\frac{\omega}{c} \left(b_\omega \exp(\mathrm{i}\omega \, t) \exp(ik \, z) - b^*_\omega \exp(-\mathrm{i}\omega \, t) \exp(-\mathrm{i}k \, z)\right) \tag{8.6}$$

is also a possible solution to Maxwell's equations. Its Poynting vector is directed along the negative z-axis. Choosing $b_\omega = a_\omega$, and using the fact that Maxwell's equations are linear,

$$E^+(z, t) + E^-(z, t) = -2\frac{\omega}{c} \sin(\omega \, t)\Big(a_\omega \exp(\mathrm{i}k \, z) + a^*_\omega \exp(-\mathrm{i}k \, z)\Big), \tag{8.7}$$

is also a possible solution. Choosing a_ω to be pure imaginary (i.e., $a_\omega = \mathrm{i}|a_\omega|$), $a_\omega + a^*_\omega = 0$, the b.c. at $z = 0$ is satisfied since,

$$E^+(0, t) + E^-(0, t) = -2\frac{\omega}{c} \sin(\omega \, t)\Big(a_\omega + a^*_\omega\Big) = 0. \tag{8.8}$$

At $z = d$

$$E^+(d,t) + E^-(d,t) = -2\omega/c\,\sin(\omega t)\,\big(a_\omega \exp(ik\,d) + a^*_\omega \exp(-ik\,d)\big) \quad (8.9)$$

which, in general, does not vanish unless the exponential factors reduce to unity. The latter condition is satisfied if $k\,d = \pi\,n$ where n is an integer, and so the wavenumber

$$k_n = \frac{\pi n}{d} \quad (8.10)$$

and the angular frequency $\omega_n = k_n c$ assume discrete values determined by the value of index n. Equation (8.7) is a *standing wave* solution illustrated in Fig. 8.1. The values of index n determine the *modes* of the cavity. The lowest frequency $\omega_0 = \pi c/d$ corresponds to mode index $n = 1$. It is called the fundamental frequency, whereas integer products of ω_0 are *harmonics* of the fundamental frequency. By adjusting the dimensions of the cavity, it is possible to tune the mode structure of the standing waves.

8.2 Cavity Quantum Electrodynamics (cQED)

Standing wave (8.9), with wavenumber (8.10), satisfies both Maxwell's equations and boundary conditions. Our goal is a quantum version of this classical description, a theory commonly called *quantum electrodynamics* or QED. Specifically, we are interested in a quantum theory for radiation trapped in the cavity, hence the moniker cavity QED, or cQED for short.

We follow the method proposed in [4] and express the standing wave solutions $E(z,t)$, $B(z,t)$, for a given mode, by the following relations

$$\begin{aligned} E(z,t) &= -\sqrt{\frac{8\pi}{L^2 d}}\,P(t)\,\sin(k_n z) \\ B(z,t) &= \sqrt{\frac{8\pi}{L^2 d}}\,\omega_n\,Q(t)\,\cos(k_n z) \\ k_n &= \frac{n\pi}{d} \qquad \omega_n = k_n c \end{aligned} \quad (8.11)$$

where $P(t)$, $Q(t)$ are real parameters. With this ansatz, Maxwell's equations require that

$$\begin{aligned} \dot{Q}(t) &= P(t) \\ \dot{P}(t) &= -\omega_n^2 Q(t), \end{aligned} \quad (8.12)$$

where the first line in (8.12) follows from condition (III) in (8.1), and the second from condition (IV).

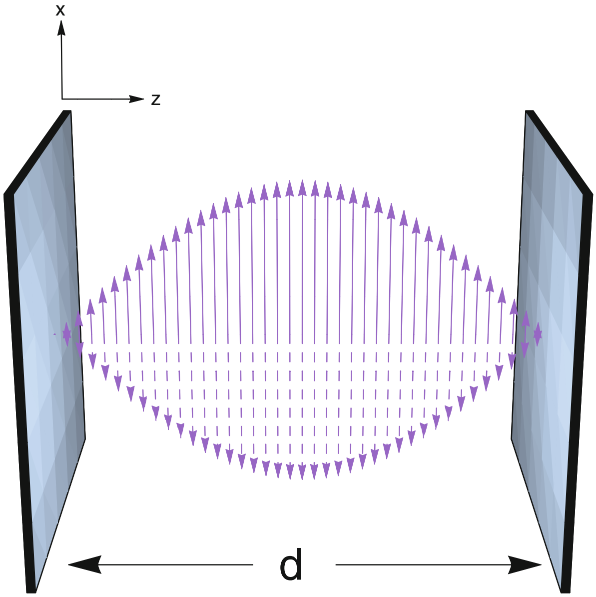

Fig. 8.1 Standing wave for the $n = 1$ mode of electric field $\vec{E}$, plane polarized along x direction. The solid line vectors represent $\vec{E}$ at $t = \pi/\omega_1$. The dashed line vectors describe the field at $t = 3\pi/\omega_1$. The standing wave oscillates in time with period $2\pi/\omega_1$ between these two extremes

They are identical to the equations obtained from Hamilton's principle if

$$H = \frac{1}{2}\left(P^2 + \omega^2 Q^2\right), \tag{8.13}$$

since

$$\frac{\partial H}{\partial P} = \dot{Q} \quad \frac{\partial H}{\partial Q} = -\dot{P}.$$

The energy content of an electromagnetic field in a box of volume $V = L^2 d$ is given by the expression [1]

$$E = \frac{1}{8\pi}\int dV\,\left(\vec{E}\cdot\vec{E} + \vec{B}\cdot\vec{B}\right), \tag{8.14}$$

where the integral is over the volume of the box. In the region bounded by the capacitor plates, whose dimension L is much greater than the spacing distance d between the plates, we find that, using (8.11),

$$E = \frac{1}{2}\left(P^2(t) + \omega_n^2\, Q^2(t)\right) = \frac{\omega_n^2}{2}\, A^2. \tag{8.15}$$

The second identity follows from the SHO solutions to (8.12)

$$Q(t) = A\,\cos(\omega_n t + \phi) \quad P(t) = -\omega_n\,A\,\sin(\omega_n t + \phi),$$

where A, ϕ are constants. The total energy in this box is constant and whose value is given by Hamiltonian (8.13), In other words, parameters P, Q are conjugate variables whose time development is governed by Hamiltonian (8.13).

Mathematica Notebook 8.1: Standing electromagnetic waves in a cavity and the Fabry-Perot interferometer. http://www.physics.unlv.edu/%7Ebernard/MATH_book/Chap8/chap8_link.html

We arrive at a quantum theory by elevating the canonical variables P, Q to quantum variables so that

$$\begin{aligned} Q \to \mathbf{Q} \quad P \to \mathbf{P} \\ [\mathbf{Q}, \mathbf{P}] = \mathrm{i}\,\hbar. \end{aligned} \tag{8.16}$$

With commutation relation (8.16), operators

$$\begin{aligned} \mathbf{a}_n &\equiv \frac{1}{\sqrt{2\hbar\omega_n}}\,(\mathbf{P} - \mathrm{i}\omega_n\,\mathbf{Q}) \\ \mathbf{a}_n^\dagger &\equiv \frac{1}{\sqrt{2\hbar\omega_n}}\,(\mathbf{P} + \mathrm{i}\omega_n\,\mathbf{Q}) \end{aligned} \tag{8.17}$$

obey

$$\left[\mathbf{a}_n, \mathbf{a}_n^\dagger\right] = 1 \tag{8.18}$$

and Hamiltonian,

$$\mathbf{H}_0 = \frac{1}{2}\left(\mathbf{P}^2 + \omega_n^2\,\mathbf{Q}^2\right) = \hbar\omega_n\left(\mathbf{a}_n^\dagger\mathbf{a}_n + 1/2\right). \tag{8.19}$$

Once again, we are led to the quantum theory of a SHO. Operators $\mathbf{a}_n$, $\mathbf{a}_n^\dagger$ are destruction and creation operators for a quantum excitation of the electromagnetic field. We call this excitation a *cavity photon*, as it corresponds to a well defined energy $\hbar\omega_n$. Hamiltonian (8.19) and the commutation relations for $\mathbf{a}_n$, $\mathbf{a}_n^\dagger$ are identical to that of phonon excitations described in the previous chapter. A single cavity photon, in mode n, is described by state

$$\mathbf{a}_n^\dagger \left|\emptyset\right\rangle,$$

and N photons by the state

$$\left|\Psi_n\right\rangle = \frac{1}{\sqrt{N!}}(\mathbf{a}_n{}^\dagger)^N \left|\emptyset\right\rangle = \frac{1}{\sqrt{N!}} \underbrace{\mathbf{a}_n^\dagger \ldots \mathbf{a}_n^\dagger}_{\text{N times}} \left|\emptyset\right\rangle, \tag{8.20}$$

where $\mathbf{a}_n \left|\emptyset\right\rangle = 0$. $\left|\Psi_n\right\rangle$ is an eigenstate of $\mathbf{H}_0$ so that

$$\mathbf{H}_0 \left|\Psi_n\right\rangle = \hbar\omega_n(N + 1/2) \left|\Psi_n\right\rangle.$$

Because Maxwell's equations are linear, the most general Hamiltonian is a sum of Hamiltonians for each mode, i.e.

$$\mathbf{H}_{em} = \sum_m \hbar\omega_m(\mathbf{a}_m^\dagger \mathbf{a}_m + 1/2) \tag{8.21}$$

where $\mathbf{a}_m^\dagger$, $\mathbf{a}_m$ are the corresponding creation and destruction operators for mode m, and obey commutation relations

$$\left[\mathbf{a}_n, \mathbf{a}_m^\dagger\right] = \delta_{nm} \quad \left[\mathbf{a}_n^\dagger, \mathbf{a}_m^\dagger\right] = [\mathbf{a}_n, \mathbf{a}_m] = 0. \tag{8.22}$$

The vacuum state $\left|\emptyset\right\rangle$ is defined so that

$$\mathbf{a}_m \left|\emptyset\right\rangle = 0 \tag{8.23}$$

for all values of m. Ket

$$\left|\Psi\right\rangle = \frac{1}{\sqrt{N_n!N_m!\ldots N_k!}}(\mathbf{a_n}{}^\dagger)^{N_n}(\mathbf{a_m}{}^\dagger)^{N_m} \ldots (\mathbf{a_k}{}^\dagger)^{N_k} \left|\emptyset\right\rangle \tag{8.24}$$

describes a state where N_m cavity photons are in mode m, N_n in mode n and N_k in mode k.

In applications, it is desirable to have a single photon occupy the cavity. In that case the system is in state $\left|\nu_n\right\rangle \equiv \mathbf{a}_n^\dagger \left|\emptyset\right\rangle$, for mode n, and the mean square value of the electric field, is given by the expectation value

$$< \vec{\mathbf{E}} \cdot \vec{\mathbf{E}} > \equiv \left\langle \nu_n \right| \vec{\mathbf{E}} \cdot \vec{\mathbf{E}} \left|\nu_n\right\rangle. \tag{8.25}$$

Using the expression (8.11) for $\vec{E}$ and the relation

$$\vec{\mathbf{E}} = -\sqrt{\frac{8\pi}{L^2 d}}\,\vec{\mathbf{P}} \sin k_n z, \quad \vec{\mathbf{P}} = \sqrt{\frac{\hbar\omega_n}{2}}\left(\mathbf{a}_n^\dagger + \mathbf{a}_n\right)\hat{\mathbf{i}}$$

(8.25) reduces to

$$\hbar\omega_n \frac{4\pi}{L^2 d} \sin^2(k_n z) \langle \nu_n | (\mathbf{a}_n^\dagger + \mathbf{a}_n)^2 | \nu_n \rangle = \hbar\omega_n \frac{12\pi}{L^2 d} \sin^2(k_n z), \tag{8.26}$$

and is proportional to the average electric field energy density (energy/volume). For the lowest frequency mode $n = 1$, where $\omega_n \equiv \omega$, the electric field energy density is proportional to $\sin^2(\pi z/d)$ and has its maximum value at the center $z = d/2$ of the plates. For the sake of economy in notation, and since we restrict our discussion to a single photon mode, we ignore the mode subscripts in the expressions for the photon destruction and creation operators $\mathbf{a}$, $\mathbf{a}^\dagger$.

A qubit, typically a two-level system such as an atom, is placed at the center $z = d/2$ of the plates where it interacts with the quantized electric field. With $\vec{r}$ the position coordinate of the electric charge, the interaction energy is given by the expression

$$\Delta W \equiv -e\,\vec{r} \cdot \vec{\mathbf{E}} = -e\,\mathbf{x}\,\mathbf{E}(d/2) = e\,\mathbf{x} \sqrt{\frac{4\pi}{L^2 d}} \sqrt{\hbar\omega}\,(\mathbf{a} + \mathbf{a}^\dagger) \tag{8.27}$$

where $\mathbf{x}$ is the quantum operator associated with the x coordinate of the electron. Let's assume that the atom is represented by a rotor situated along the xz plane of Fig. 8.1. Using the matrix representation for the rotor-electron operator $\mathbf{x} = R/2\boldsymbol{\sigma}_X$, we obtain

$$\begin{aligned} \Delta W &= \hbar\,\Omega\,\boldsymbol{\sigma}_X \left(\mathbf{a} + \mathbf{a}^\dagger\right) = \\ \Omega &= eR\sqrt{\frac{\pi\omega}{V\hbar}} \end{aligned} \tag{8.28}$$

where R is the rotor radius and $V = dL^2$ is the volume of the cavity confined by the capacitor plates. Including Hamiltonian (7.25) for the rotor, and (8.19) for the single mode cavity photons, the interacting atom (rotor)—cavity photon Hamiltonian is

$$\begin{aligned} \mathbf{H} &= \mathbf{h}_0 + \hbar\omega(\mathbf{a}^\dagger\mathbf{a} + 1/2) + \hbar\,\Omega\,\boldsymbol{\sigma}_X \left(\mathbf{a} + \mathbf{a}^\dagger\right) \\ \mathbf{h}_0 &= -\frac{\hbar\,\omega_0}{2}\boldsymbol{\sigma}_Z. \end{aligned} \tag{8.29}$$

In the interaction picture, these time-independent operators become time-dependent operators via the prescription

$$\begin{aligned} \mathbf{a} &\to \exp(\mathrm{i}\,\mathbf{H}_0\,t/\hbar)\,\mathbf{a}\,\exp(-\mathrm{i}\,\mathbf{H}_0\,t/\hbar) = \mathbf{a}\,\exp(-\mathrm{i}\,\omega\,t) \\ \mathbf{a}^\dagger &\to \exp(\mathrm{i}\,\mathbf{H}_0\,t/\hbar)\,\mathbf{a}^\dagger\,\exp(-\mathrm{i}\,\mathbf{H}_0\,t/\hbar) = \mathbf{a}^\dagger\,\exp(\mathrm{i}\,\omega\,t) \end{aligned} \tag{8.30}$$

also

$$\boldsymbol{\sigma}_X \to \exp(\mathrm{i}\,\mathbf{h}_0\,t/\hbar)\,\boldsymbol{\sigma}_X\,\exp(-\mathrm{i}\,\mathbf{h}_0\,t/\hbar) = \exp(\mathrm{i}\,\mathbf{h}_0\,t/\hbar)(\sigma_+ + \sigma_-)\exp(-\mathrm{i}\,\mathbf{h}_0\,t/\hbar)$$
$$\to \sigma_+\exp(\mathrm{i}\,\omega_0\,t) + \sigma_-\exp(-\mathrm{i}\,\omega_0\,t), \tag{8.31}$$

and the product

$$\boldsymbol{\sigma}_X\left(\mathbf{a}+\mathbf{a}^\dagger\right) \to$$
$$(\sigma_+\exp(\mathrm{i}\,\omega_0\,t) + \sigma_-\exp(-\mathrm{i}\,\omega_0\,t))\left(\mathbf{a}\,\exp(-\mathrm{i}\,\omega\,t) + \mathbf{a}^\dagger\exp(\mathrm{i}\,\omega\,t)\right). \tag{8.32}$$

Expanding (8.32) we find terms proportional to $\exp(\pm\mathrm{i}(\omega+\omega_0)t)$ and $\exp(\pm\mathrm{i}(\omega-\omega_0)t)$. Close to resonance where $\omega \approx \omega_0$, it is only the latter terms that contribute in the RWA approximation. Therefore, we are allowed to replace (8.28) with operator

$$\hbar\,\Omega\,\left(\mathbf{a}\,\sigma_+ + \mathbf{a}^\dagger\,\sigma_-\right).$$

In this approximation we obtain the *Jaynes-Cummings Hamiltonian* [4], a workhorse of cQED,

$$\mathbf{H}_{JC} = -\frac{\hbar\omega_0}{2}\boldsymbol{\sigma}_Z + \hbar\omega(\mathbf{a}^\dagger\mathbf{a} + 1/2) + \hbar\,\Omega\,\left(\mathbf{a}\,\sigma_+ + \mathbf{a}^\dagger\,\sigma_-\right). \tag{8.33}$$

Indeed, we already met $\mathbf{H}_{JC}$ in the trapped-ion scenario discussed in Chap. 7. There, a SHO Hamiltonian describes the spectrum of phonon excitations, i.e., the "phonon bus", and here, cavity photons assume the role of the "bus". With photon-atom coupling, we can shuttle quantum information from qubits to cavity photons, and vice-versa [2].

8.2.1 Eigenstates of the Jaynes-Cummings Hamiltonian

We seek energy eigenstates of Hamiltonian (8.33), i.e., solutions to

$$\mathbf{H}_{JC}\,|\phi\rangle = E_n\,|\phi\rangle\,. \tag{8.34}$$

To that end it is useful to define the states

$$|n,\,0\rangle \equiv |n\rangle\otimes|0\rangle \qquad |n,\,1\rangle \equiv |n\rangle\otimes|1\rangle \tag{8.35}$$

where $|0\rangle\,,|1\rangle$ are atomic(rotor) qubit states, $|n\rangle$ the eigenstates of Hamiltonian $\hbar\omega(\mathbf{a}^\dagger\mathbf{a} + 1/2)$, and n is the photon occupation number. The cavity is tuned to near resonance so that $\hbar\omega \approx \hbar\omega_0$ and states $|\phi_0\rangle \equiv |n,\,0\rangle$, $|\phi_1\rangle \equiv |n-1,\,1\rangle$ are nearly degenerate. For approximate solutions to (8.34), we posit the ansatz

$$|\phi\rangle = c_1 |\phi_0\rangle + c_2 |\phi_1\rangle , \tag{8.36}$$

and construct the matrix representation of the Jaynes-Cummings Hamiltonian with basis $|\phi_0\rangle$, $|\phi_1\rangle$. Thus

$$\underline{\text{H}}_{JC} = \begin{pmatrix} \langle\phi_0| \mathbf{H}_{JC} |\phi_0\rangle & \langle\phi_0| \mathbf{H}_{JC} |\phi_1\rangle \\ \langle\phi_1| \mathbf{H}_{JC} |\phi_0\rangle & \langle\phi_1| \mathbf{H}_{JC} |\phi_1\rangle \end{pmatrix} = \begin{pmatrix} \hbar\omega_0 n & \hbar\Omega\sqrt{n} \\ \hbar\Omega\sqrt{n} & \hbar\omega_0 n \end{pmatrix}, \tag{8.37}$$

where we used the fact that $\mathbf{a}^\dagger |n\rangle = \sqrt{n+1}\,|n\rangle$. With ansatz (8.36) we obtain the matrix representation of eigenvalue Eq. (8.34)

$$\begin{pmatrix} \hbar\omega_0 n & \hbar\Omega\sqrt{n} \\ \hbar\Omega\sqrt{n} & \hbar\omega_0 n \end{pmatrix} \begin{pmatrix} c_1 \\ c_2 \end{pmatrix} = E \begin{pmatrix} c_1 \\ c_2 \end{pmatrix} \tag{8.38}$$

whose eigenvalues are

$$E_\pm = \hbar\omega_0 n \pm \hbar\Omega\sqrt{n} \tag{8.39}$$

corresponding to eigenstates

$$\begin{aligned} |\phi_+\rangle &= \frac{1}{\sqrt{2}} \left(|n, 0\rangle + |n-1, 1\rangle\right) \\ |\phi_-\rangle &= \frac{1}{\sqrt{2}} \left(|n, 0\rangle - |n-1, 1\rangle\right) \end{aligned} \tag{8.40}$$

respectively. Suppose a qubit in the ground state $|0\rangle$ is introduced into a cavity containing n-single mode photons at $t = 0$. The Jaynes-Cummings Hamiltonian predicts that the composite system evolves, for $t > 0$, according to

$$\begin{aligned} &|\psi(t)\rangle = \exp(-\mathrm{i}\mathbf{H}_{JC}t/\hbar)\,|n, 0\rangle = \\ &\exp(-\mathrm{i}\omega_0 n\, t)\left(\cos(\Omega\sqrt{n}\, t)\,|n, 0\rangle - \mathrm{i}\sin(\Omega\sqrt{n}\, t)\,|n-1, 1\rangle\right). \end{aligned} \tag{8.41}$$

Equation (8.41) predicts a probability to find n photons in the cavity, and which oscillates between the photon number n and $n-1$ with a period determined by Ω and $\sqrt{n}$. It is yet another manifestation of coherent Rabi-flopping. Energy quanta are exchanged between the qubit and the electromagnetic field. Unlike Rabi-flopping of a single qubit, cQED features flopping of entangled states of the qubit and photons.

Laboratory demonstrations of *Rydberg atom* qubits interacting with cavity photons have verified the existence of the predicted oscillations. In *S. Haroche's* laboratory [2], a cavity comprised of a high-Q reflecting material confined single mode photons for as long as 130 ms. It translates, given the dimensions of the cavity, to a total transit distance of 40,000 km as the photon bounces back and forth billions of times. At the same time Rydberg atoms whose qubits states are separated by an energy defect corresponding to $2\pi\omega_0 = 51\,\mathrm{GHz}$, are introduced into the nearly resonant cavity. By using a method called non-demolition measurements, the group was able to measure the cavity photon number after transit of the Rydberg atom qubit. Measurements revealed the predicted oscillations in photon number as a function of atom-cavity transit time t and confirmed the predicted strong-coupling of an atom/ion with a quantized field. S. Haroche and D. Wineland shared the 2012 Nobel prize in physics for their pioneering work in the domain of cavity QED and ion-trap demonstrations respectively. In the Nobel committee statement, they were cited *"for ground-breaking experimental methods that enable measuring and manipulation of individual quantum systems", and "Their ground-breaking methods have enabled this field of research to take the very first steps towards building a new type of super fast computer based on quantum physics."*

8.3 Circuit QED (cirQED)

A descendant of cavity QED, circuit QED or cirQED, shows great promise as a quantum computing and information platform. In a span of a dozen years or so, cirQED has positioned itself from a dark-horse to a leading contender. Instead of atoms, cirQED employs "artificial atoms" for its qubits and which are best described with electronic circuit terminology. In cirQED, microwave photons supported by planar superconducting transmission lines, or excitations of a superconducting circuit operating at the quantum limit, serve the role of the cavity photon "bus" in cQED.

8.3.1 Quantum LC Circuits

Let's consider an electrical circuit that consists of conducting elements, such as a *capacitor* and *inductor* connected in series (see Fig. 8.2 panel (a)). A capacitor consists of two conductors that are separated, on which equal but opposite signed charges $\pm Q$ reside. Those charges support an electric field in the space between the conductors and, in turn, leads to a voltage difference ΔV_C between the positive and negative charged plates. It turns out that the ratio of charge Q and ΔV_C is always constant so that

$$Q/\Delta V_C = C \tag{8.42}$$

where C is called the capacitance. The *SI* unit of capacitance is called the *Farad*, or F, after the nineteenth century electro-magnetism pioneer *Michael Faraday*. Capacitors store electric field energy and are found in a wide array of electric circuit applications. Another common component in electric circuits, an inductor, stores magnetic energy. The generic inductor is a conducting wire configured into a solenoid loop. As current winds around the loop, a magnetic field is set-up inside and along the axis of the solenoid. If the magnetic field changes in time due a time dependent current, the *Faraday induction law* stipulates that the circuit responds with an induced electric field. The latter sets up a voltage difference between the endpoints, or ports, of the inductor. Faraday's law provides a precise relationship between the voltage ΔV_L difference and the time derivative of the current passing through the solenoid. If $I_{ab}(t)$ is the current traversing from terminal a to terminal b of a solenoid

$$\Delta V_L = -L\frac{dI_{ab}}{dt}$$
$$\Delta V_L \equiv V_b - V_a. \tag{8.43}$$

The constant L is called the *inductance* of the circuit and is expressed in units of

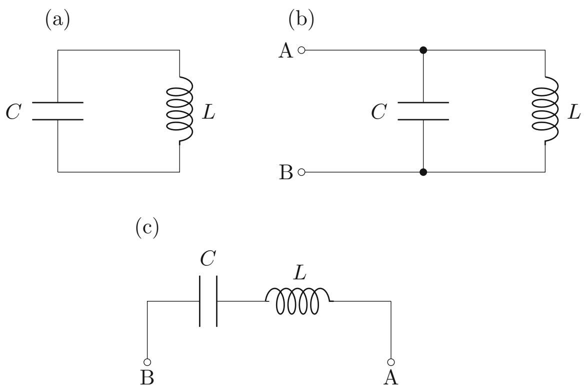

Fig. 8.2 Circuit diagrams for an LC. Circuit. Panel (**a**) is a stand-alone LC circuit. Panels (**b**) and (**c**) illustrate LC circuits containing ports that allow coupling to an external voltage source

Henry, or H, after *Joseph Henry*. When the conducting leads of each capacitor plate are connected, so that the circuit is closed, current flows to neutralize the charge separation between the capacitor plates. Without an inductor, neutralization occurs in a minuscule fraction of a second. With an inductor along the current path, a counteracting potential prevents neutralization of the circuit. In the initial stages of the discharge, the current increases in the inductor thereby increasing the magnetic flux. The increasing magnetic flux reverses, because of induction, the voltage polarity of the inductor. This scenario, in which electric and magnetic energy is being shuttled back and forth between capacitor and inductor, is best expressed mathematically. Since the current in the wire is the negative of the time rate of change of the charge Q on the capacitor

$$I(t) = -\frac{dQ(t)}{dt}$$

and assuming that outside each lumped circuit element the magnetic flux vanishes, we appeal to the *Kirchoff loop law* [1], $\Delta V_C + \Delta V_L = 0$, or

$$\frac{Q(t)}{C} = L\,\dot{I}(t)$$
$$\dot{Q}(t) = -I(t), \tag{8.44}$$

The second equation follows from the definition of current and we used the dot notation for time derivatives. It is convenient to express (8.44) in terms of $\Phi(t) \equiv -L\,I(t)$, the magnetic flux associated with the inductor, and so

$$\frac{Q(t)}{C} = -\dot{\Phi}(t)$$
$$\frac{\Phi(t)}{L} = \dot{Q}(t). \tag{8.45}$$

Let's define the Hamiltonian

$$H = \frac{\Phi^2}{2L} + \frac{Q^2}{2C} \tag{8.46}$$

where Φ is the conjugate momentum to variable Q. Hamilton's equations lead to the expressions

$$\frac{\partial H}{\partial \Phi} = \dot{Q} \Rightarrow \frac{\Phi}{L} = \dot{Q}$$
$$\frac{\partial H}{\partial Q} = -\dot{\Phi} \Rightarrow \frac{Q}{C} = -\dot{\Phi}, \tag{8.47}$$

that are in harmony with (8.45).

Quantization of (8.46) proceeds by replacing the classical variables Φ, Q with their quantum operators that obey the quantization rule $[\boldsymbol{\Phi}, \mathbf{Q}] = -\mathrm{i}\hbar$. Defining the operators

$$\mathbf{a} = \sqrt{\frac{Z_0}{2\hbar}}\left(\mathbf{Q} + \mathrm{i}\,\frac{\boldsymbol{\Phi}}{Z_0}\right)$$
$$\mathbf{a}^\dagger = \sqrt{\frac{Z_0}{2\hbar}}\left(\mathbf{Q} - \mathrm{i}\,\frac{\boldsymbol{\Phi}}{Z_0}\right)$$
$$Z_0 \equiv \sqrt{\frac{L}{C}} \tag{8.48}$$

we find that $\left[\mathbf{a}, \mathbf{a}^\dagger\right] = 1$ and

$$\mathbf{H} = \hbar\omega\left(\mathbf{a}^{\dagger}\mathbf{a} + 1/2\right)$$
$$\omega = \frac{1}{\sqrt{LC}}. \quad (8.49)$$

We arrived at yet another example involving a simple harmonic oscillator model description. In Chap. 7, a SHO Hamiltonian (7.62) described vibrational excitation about an equilibrium configuration of interacting ions. Equation (8.19) posits a SHO model for quantum excitations of the electromagnetic field in a cavity. Above, (8.49) describes the quantum excitation of a current in an LC circuit. Three disparate physical systems are depicted by the SHO model, underscoring its universal utility.

With advances in the microelectronic engineering of *superconducting* elements, LC circuits exhibiting quantum behavior have been realized in the laboratory. An essential feature of superconducting micro LC circuits is the lack of dissipation, i.e., the circuit does not contain resistive elements that drain and convert electric and magnetic energy into heat. Under ordinary conditions, perfect conductors (without dissipation) do not exist, but a superconductor can sustain a current without significant dissipation. Therefore, microelectronic superconducting LC circuits operating in the quantum regime can serve as a "bus" in quantum processing applications. Because quantum LC circuits, photons, and phonons are all described by the SHO model, a common theoretical framework is available. The converse is also true; we can model cavity photons as excitations of an LC circuit.

Superconductivity, a phenomenon characterized by the apparent loss of resistivity that allows the persistence of electric current, was discovered in 1911 by *Heike Kamerlingh Onnes*. Superconductivity also displays the *Meissner effect*, the rejection of magnetic fields in the transition from an ordinary conduction state to a superconductor. Materials that exhibit super-conduction do so at extremely low temperatures, typically at temperatures where helium gas becomes liquid, i.e., at around 4 K. One Kelvin is equivalent to about $-272.15\,^{\circ}$C. In the past 30 years or so a new class of materials displaying superconductivity at around 100 K had been discovered. Fittingly, the phenomenon is called high-T_c superconductivity. However, those materials have not yet found widespread application in electronic circuitry.

In a micro-circuit with capacitance $C = 10^{-11}$ F and inductance $L = 10^{-9}$ H, the quanta of energy is given by the expression

$$\hbar\omega = \hbar\frac{1}{\sqrt{LC}} = 1.05 \times 10^{-24}\,\mathrm{J}$$

where J denotes the Joule, the SI unit of energy. Lets compare this figure of merit with $k_B T$, where k_B is the *Boltzmann constant*, the ambient energy that characterizes the environment. Or

$$T = \hbar\omega/k_B \approx 80\,\mathrm{mK}.$$

At temperatures above this threshold exposure of the LC oscillator with the environment threatens coherence and tends to classical behavior. Clearly, a viable QCI platform based on present day superconducting technology requires a very cold environment.

To build quantum gates we need to couple the LC circuits to qubits. In the terminology of electronic circuit theory, this is accomplished by terminals or ports, connected, as illustrated in Fig. 8.2, to the LC circuit. Typically, a time-dependent voltage difference $V(t)$ across the ports drives current $I(t)$. We assume the time dependence is sinusoidal so that

$$V(t) = Re(v \exp(j\,\omega\,t)) \quad I(t) = Re(i\ \exp(j\omega\,t)), \tag{8.50}$$

(Note: in this section, we use the electrical engineering convention in which the imaginary number i is replaced by the symbol j) where v, i are complex numbers, ω is a driving frequency, and Re represent the real part of these expressions. For linear circuits, v is related to i via the relationship

$$v = i\,Z \tag{8.51}$$

where Z is a complex number and is called the *circuit impedance*. In a lumped circuit $\partial\vec{B}/\partial t$ is assumed to vanish in regions of the circuit that are external to the circuit elements, including capacitors, inductors, and resistors. Each is characterized by an element impedance, defined according to the rules [1]

$$Z_C = \frac{1}{j\,\omega\,C} \quad Z_L = j\omega\,L \quad Z_R = R. \tag{8.52}$$

Here Z_C, Z_L, Z_R are impedances for a capacitor with capacitance C, inductor with inductance L, and resistor with resistance R. For a circuit with elements connected in series, as in panel (c) of Fig. 8.2, the effective impedance Z of the circuit is the sum

$$Z = Z_1 + Z_2 + Z_3 + \dots$$

where Z_i is the impedance of element i. If the elements are connected in parallel, as in panel (b) of Fig. 8.2,

$$\frac{1}{Z} = \frac{1}{Z_1} + \frac{1}{Z_2} + \frac{1}{Z_3} + \dots$$

So for an LC circuit, with negligible resistance, connected in series

$$Z = \frac{1}{j\,\omega\,C} + j\,\omega L = -j\,\frac{1-\omega^2 L\,C}{\omega C} = (X_C - X_L)\exp(-j\,\pi/2)$$

where $X_C \equiv 1/\omega C$, $X_L \equiv \omega L$ are the capacitance and inductive reactance respectively. Inserting this expression into (8.51) we find that

$$I(t) = \frac{1}{X_C - X_L} \cos(\omega t + \pi/2 + \phi_0) \tag{8.53}$$

where $v = V \exp(j\phi_0)$ and V is real. If the driving frequency ω is close to $\omega_0 = 1/\sqrt{LC}$, the natural or resonance frequency of the LC circuit, the current $I(t)$ approaches its maximum value. At resonance $\omega = \omega_0$, expression (8.53) is undefined, but if we include a non-vanishing resistance R, we obtain

$$I(t) = V/R \cos(\omega_0 t + \phi_0)$$

at resonance.

Mathematica Notebook 8.2: An Introduction to Transmission Line resonators. http://www.physics.unlv.edu/%7Ebernard/MATH_book/Chap8/chap8_link.html

8.3.2 Artificial Atoms

In one version of cirQED [3], a microwave transmission line resonator serves as the analog of a cQED cavity. But, we also need the circuit analog of a qubit to develop QCI capabilities. Unlike an atom/ion, the quantum energy defects in an LC circuit are uniform and so are not suitable qubit candidates. In cirQED, a qubit is realized with circuits containing *Josephson junctions* (JJ), after *Brian Josephson* who first predicted their behavior in the 1960s. Circuits containing Josephson junctions are built to exhibit atom/ion-like features and, therefore, have also been called artificial atoms.

Superconductivity is an inherently quantum mechanical effect, but unlike atoms, molecules and other familiar systems that exhibit quantum behavior, superconductivity is a macroscopic phenomenon. A conductor supports about 10^{22} conduction electrons per cubic cm, but in the superconducting state, they exhibit coherent behavior by forming so-called *Cooper pairs*, after *F. Cooper*, who along with colleagues *Bardeen*, and *Schrieffer* developed the modern low-temperature theory of superconductivity, also know as the *BCS* theory. The theory posits that electrons behave as a coherent collective entity much like a wave, rather than individual classical billiard-like objects. Though the BCS theory is beyond the scope of our discussion, we will rely on a more accessible phenomenological description that allows us to predict the behavior of currents and charges near a Josephson junction.

At its most fundamental level, a Josephson junction consists of two superconducting wires separated by a small gap filled by some non-conducting material that cannot be bridged by ordinary currents. That sounds like a description for a capacitor, and the Josephson junction does have an intrinsic capacitance but, unlike a standard capacitor, Cooper pairs with charge $2\,e$ can bridge the gap by a process called *tunneling*. The latter is a common feature in quantum systems, but for our purposes, we need not concern ourselves with details of tunneling theory, as long as we accept it as a phenomenological fact.

8.3.3 Superconducting Qubits

Let n_a, n_b represent the number of Cooper pairs on superconducting wires a, b that form the boundary of the junction. We define phase parameters δ_a, δ_b for the corresponding regions. These parameters arise from the need to describe the electron gas by a quantum mechanical wave amplitude. For example, in our discussion of the quantum rotor system, the wave amplitude was written in the form (7.17) which includes a magnitude and a phase. Here the amplitude $\psi \sim \sqrt{n}\exp(\mathrm{i}\delta)$ describes the collective behavior of electron pairs in a superconductor. The JJ is characterized by the variables

$$\delta \equiv \delta_b - \delta_a \quad Q = 2e(n_a - n_b)$$

where Q represents the excess charge and δ the phase difference across a junction. In applying the BCS theory, Brian Josephson derived the following equations

$$\begin{aligned} \dot{\delta} &= \frac{2e\,V}{\hbar} \\ I &= I_0 \, \sin\delta \end{aligned} \tag{8.54}$$

where $I(t)$ is the current (or supercurrent) flowing across the junction, $V(t)$ the voltage difference across the junction and $I_0 = E_J\,2e/\hbar$ is a constant. The quantity E_J is the Josephson energy, a measure of junction characteristics. Since the junction also acts as a capacitor, $V = Q/C$ and $I = -\dot{Q}$, and we re-write (8.54) in the form

$$\begin{aligned} \dot{\delta} &= \frac{2e\,Q}{\hbar\,C} \\ \dot{Q} &= -I_0 \, \sin\delta \end{aligned} \tag{8.55}$$

where C is the capacitance of the junction. In typical junctions, C is on the order of 10^{-12} F and I_0 on the order of $10\,\mu$A (A is an Ampere, the SI unit for current). We define an effective Hamiltonian $H_{JJ}(Q, \Phi)$

$$H_{JJ}(Q, \Phi) = E_C\,(\frac{Q}{e})^2 + E_J(1 - \cos(\Phi/\Phi_0)).$$
$$E_C \equiv \frac{e^2}{2C} \quad \Phi_0 \equiv \frac{\hbar}{2e} \tag{8.56}$$

where $\Phi = \Phi_0\,\delta$ is a generalized coordinate and Q its conjugate momentum. From Hamilton's equations

$$\frac{\partial H_{JJ}}{\partial Q} = \dot{\Phi} \quad \frac{\partial H_{JJ}}{\partial \Phi} = -\dot{Q}$$

it follows that

$$\frac{2E_C Q}{e^2} = \Phi_0 \dot{\delta}$$

$$\frac{E_J}{\Phi_0}\,\sin(\Phi/\Phi_0) = -\dot{Q}, \tag{8.57}$$

which when substituting the definitions for E_C, Φ_0 is identical to the Josephson equations (8.55).

Mathematica Notebook 8.3: Eigenstates of a Josephson junction. http://www.physics.unlv.edu/%7Ebernard/MATH_book/Chap8/chap8_link.html

Suppose we are in the regime in which $\Phi/\Phi_0 < 1$ and it is legitimate to express $\cos(\Phi/\Phi_0)$ as a power series in Φ/Φ_0. We then obtain

$$H_{JJ} = H^0_{JJ} + H_{NL}$$
$$H^0_{JJ} = \frac{Q^2}{2C} + \frac{\Phi^2}{2L_J} \tag{8.58}$$

where H_{NL} consists of all terms beyond second order in the power expansion of the argument, and

$$L_J \equiv \frac{\Phi_0}{I_0}$$

is a self-inductance. H^0_{JJ} describes a SHO whereas H_{NL} is an anharmonic correction. The latter term allows JJ circuits to function as viable qubits. Because H_{NL} introduces anharmonicity, as shown in Fig. 8.3, to the harmonic potential

$$V_{SHO} = \frac{\Phi^2}{2L_J}$$

the energy eigenvalue defects of H_{JJ} are not equally spaced. We express a system governed by H_{JJ} with the circuit shown in Fig. 8.4. In that figure the elements

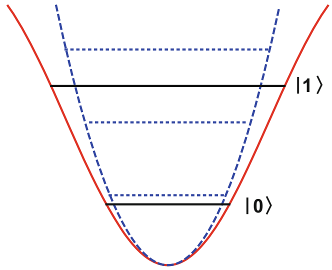

Fig. 8.3 Artificial atom qubit energy spectrum for Hamiltonian (8.58). States $|0\rangle$, $|1\rangle$ denote the qubit states, whereas the dotted lines are, uniformly spaced, energy eigenstates of H^0_{JJ}. The dashed curve represents V_{SHO}, whereas the solid curve includes the anharmonic contribution H_{NL}

corresponding to the JJ capacitance and self-inductance are connected in parallel to the element denoted by the spider symbol. The latter is a non-linear circuit component that represents the anharmonic contribution H_{NL} in Hamiltonian (8.58). Together they constitute an equivalent circuit containing only a single element, represented by the boxed cross symbol in Fig. 8.4.

Mathematica Notebook 8.4: Charge, Phase and Flux artificial atom qubits. http://www.physics.unlv.edu/%7Ebernard/MATH_book/Chap8/chap8_link.html

In QCI applications it is desirable to have the JJ qubit coupled to a LC "bus." There are several ways of doing this, one of which is illustrated in Fig. 8.5. In that figure, a JJ qubit is connected to a LC circuit via two capacitors. It can be shown [6] that the Hamiltonian describing it is similar to the Jaynes-Cummings Hamiltonian discussed in the previous section. There we noted how the eigenstates of the latter exhibit entanglement between qubit and photon states. Analogously, we expect entanglement of the JJ qubit with resonator quanta.

The system described by the circuit illustrated in (8.5) is somewhat simplistic. In laboratory realizations, circuit involving non-linear JJ elements are coupled to a complex network of linear elements, e.g., capacitors, resistors, and inductors. As shown in the previous section, such a network is conveniently described by its impedance. Knowing that a Josephson junction is equivalent to the circuit shown in Fig. 8.4, we re-express the circuit in Fig. 8.5 with that shown in panel (a) of Fig. 8.6. In it, we collected all linear elements, circumscribed by the dashed line, and replaced them with a "black box" characterized by a single parameter, the black box impedance $Z(\omega)$ expressed as a function of the driving frequency ω. The non-linear JJ element is coupled, as shown in panel (b) of Fig. 8.6, to the box. In a procedure called *black-box quantization* [5], or BBQ for short, knowledge of $Z(\omega)$ allows one to predict the energy spectrum, and basis vectors associated with it, of the black box. The basis vectors can then be used to form a matrix representation, which can be diagonalized, of the nonlinear term coupled to the black box. In this way, a systematic procedure is available to find the spectrum and eigenstates for a cirQED system.

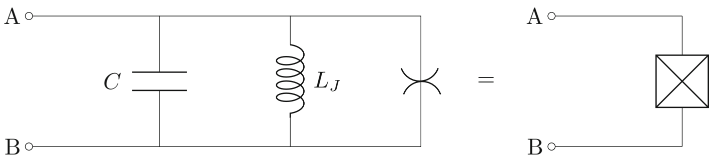

Fig. 8.4 Equivalent circuit for the JJ qubit shown by the crossed boxed symbol. We designate the non-linear component, arising from H_{NR}, with the spider symbol

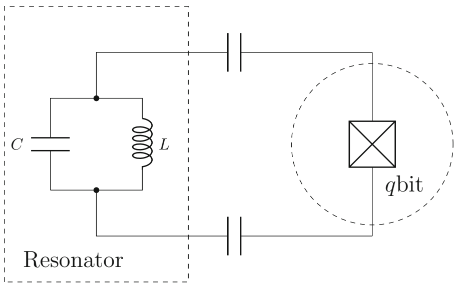

Fig. 8.5 Josephson junction qubit coupled to a resonator circuit

Problems

8.1 Demonstrate that ansatz (8.2) satisfies conditions (I), (II), (III) in (8.1).

8.2 Show that ansatz (8.2) satisfies condition (IV) in (8.1), only if $a(t)$ is a solution to (8.3).

8.3 Verify that $a(t) = a_\omega \exp(\pm \mathrm{i}\, \omega t)$ are solutions to (8.3), provided that $\omega = k\, c$.

8.4 Using definition (8.4) for the Poynting vector, and ansatz (8.2), derive relation (8.5) for the time average of the Poynting vector.

8.5 Find the time average of the Poynting vector, for field configurations (8.6) and (8.7). Comment.

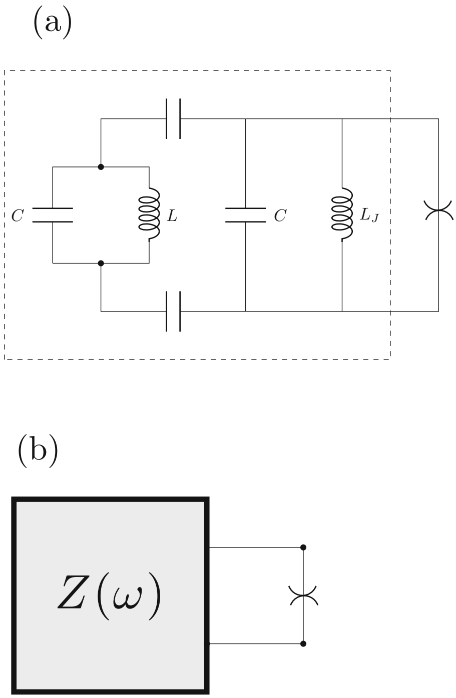

Fig. 8.6 A BBQ circuit

8.6 Show that $\vec{E}(t) = \hat{\mathbf{i}}\, E(z,t)$ and $\vec{B}(t) = \hat{\mathbf{j}}\, B(z,t)$, where $E(z,t)$, $B(z,t)$ are given by (8.11), satisfy the Maxwell equations in a vacuum.

8.7 Consider the single mode (mode index not shown) non-normalized photon state

$$|\psi\rangle = |\emptyset\rangle + \mathbf{a}^\dagger \mathbf{a}^\dagger\, |\emptyset\rangle\, .$$

Evaluate $\langle\psi|\,\psi\rangle$. (Hint: to evaluate the expectation value of operator $\mathbf{a}\,\mathbf{a}\,\mathbf{a}^\dagger\,\mathbf{a}^\dagger$, use commutation relations (8.22) to move the destruction operators toward the right so that you can exploit (8.23) and "destroy the vacuum".)

8.8 Consider the single mode (mode index not shown) photon state

$$|\psi\rangle = \frac{1}{\sqrt{2}}\Big(|\emptyset\rangle + \mathbf{a}^\dagger\, |\emptyset\rangle\Big)\, .$$

Find the expectation value $\langle\psi|\,\mathbf{N}\,|\psi\rangle$, where $\mathbf{N} = \mathbf{a}^\dagger\,\mathbf{a}$ is a photon number operator.

8.9 For the state given in problem (8.8), calculate the variance

$$\Delta\mathbf{N}^2 \equiv \langle\psi|\,\mathbf{N}^2\,|\psi\rangle - \langle\psi|\,\mathbf{N}\,|\psi\rangle^2\, .$$

8.10 For the fields defined in problem (8.6), evaluate expression (8.14) and verify relation (8.15).

8.11 Using definition (8.25) verify relation (8.26).

8.12 For $\vec{E}$ given in problem (8.6), find the expectation value

$$\langle\psi|\,\vec{\mathbf{E}}\cdot\vec{\mathbf{E}}\,|\psi\rangle$$

for the, single mode, state

$$|\psi\rangle = \frac{1}{\sqrt{2}}\mathbf{a}^{\dagger}\,|\emptyset\rangle + \frac{1}{2}\mathbf{a}^{\dagger}\mathbf{a}^{\dagger}\,|\emptyset\rangle\,.$$

The mode index of the creation operator is not shown.

8.13 Verify identities (8.30).

8.14 Using the basis states (8.35), evaluate the matrix representation of the Jaynes-Cummings Hamiltonian and verify (8.37).

8.15 Using definitions (8.40) evaluate the expectation values

$$\langle\phi_{\pm}|\,\mathbf{H}_{JC}\,|\phi_{\pm}\rangle\,.$$

8.16 Evaluate the expectation value

$$\langle\psi(t)|\,\mathbf{H}_{JC}\,|\psi(t)\rangle$$

where $|\psi(t)\rangle$ is given by (8.41).

8.17 Find the mean number of photons $\mathbf{N}$, as a function of time, for state (8.41). Evaluate the variance $\Delta\mathbf{N}^2$ for this state.

8.18 Find the matrix representation $\underline{\psi}(t)$, with respect to basis vectors (8.35), of ket (8.41). Show that it satisfies the Schroedinger equation

$$\mathrm{i}\,\hbar\frac{\partial\underline{\psi}(t)}{\partial t} = \underline{\underline{\mathbf{H}}}_{JC}\,\underline{\psi}(t),$$

where $\underline{\underline{\mathbf{H}}}_{JC}$ is given by (8.37).

8.19 Consider the circuit comprised of linear elements and shown within the dashed line in panel (a) of Fig. 8.6. Assume the unlabeled coupling capacitors in that circuit have the value $C/2$. Find the impedance of this circuit as a function of a driving term with angular frequency ω.

8.20 Evaluate the exercises in Mathematica Notebook 8.3.

References

1. Richard P. Feynman, Robert B Leighton, Matthew Sands, *Feynman Lectures in Physics, Vol. II* Addison-Wesley, 1965
2. Serge Haroche, Reviews of Modern Physics, **85**, 1083 2013
3. S. Girvin, in *Quantum machines: Measurement and Control of Engineered Quantum Systems: Lecture Notes of the Les Houches Summer School*, ed. by Michel Devoret, Benjamin Huard, Robert Schoelkopf, and Leticia F. Cugliandolo, Volume 96, (Oxford Scholarship Online, 2014).
4. Edwin T. Jaynes, Frederick W Cummings, Proceedings of the IEEE, 51, 89 1963
5. Simon E. Nigg, Hanhee Paik, Brian Vlastakis, Gerhard Kirchmair, S. Shankar, Luigi Frunzio, M. H. Devoret, R. J. Schoelkopf, and S. M. Girvin, Physical Review Letters, **108**, 240502 (2012)
6. Uri Vool and Michel Devoret, arXiv:1610.03438v2, 2017